Journal of Biomechanical Science and Engineering

Vol. 7, No. 2, 2012

Numerical Study on Platelet Adhesion to Vessel Walls using the Kinetic Monte Carlo Method*

Seiji SHIOZAKI**, Kenichi L. ISHIKAWA**,*** and Shu TAKAGI**,***

**Computational Science Research Program, RIKEN,
2-1, Hirosawa, Wako-shi, Saitama 351-0198, Japan
E-mail: shios@riken.jp

***School of Engineering, The University of Tokyo,
7-3-1, Hongo, Bunkyo-ku, Tokyo 113-8656, Japan

Abstract

The interaction between platelets and vessel walls in the primary aggregation of platelets was investigated using kinetic Monte Carlo simulation for the multiscale simulation of thrombus formation. The kinetic Monte Carlo lattice model of a platelet surface with glycoprotein Ibα (GPIbα) localization region was simulated by considering 3 types of events: GPIbα diffusion, GPIbα–von Willebrand factor (vWF) bond formation, and breakage. The formation and breakage model of GPIbα–vWF bonds were constructed to reproduce experimental results. Next, the adhesion force between a platelet and vessel wall was evaluated, and the contribution of GPIbα localization in platelet adhesion was investigated. The adhesion force curves with respect to the distance between the platelet and vessel wall were convex upward. The results showed that when the bond formation probability between GPIbα and vWF was small, the localization of GPIbα had a large effect on the adhesion force between the platelet and the vessel wall.

Key words: Thrombus Formation, Platelet Aggregation, Glycoprotein Ibα, Von Willebrand Factor, Kinetic Monte Carlo Method

1. Introduction

In the initial stage of thrombus formation, platelet aggregation occurs on the inner walls of vessels. The glycoprotein Ibα (GPIbα), which is present on the platelet surface, plays a crucial role in platelet aggregation via its interaction with von Willebrand factor (vWF). A platelet has 15000–20000 GPIbα molecules on its surface[(1)-(3)]. When the endothelial cells on the vascular surface are damaged, vWF instantly binds to the exposed subendothelial tissues. Platelets can adhere to the vessel wall via an interaction between the vWF A1 domain (vWFA1) and the platelet GPIbα N-terminal. The GPIbα–vWFA1 bond has a short lifetime and cannot adhere irreversibly by itself. In the contact region between a platelet and vessel wall, multiple GPIbα–vWFA1 bonds are formed, and the number of bonds varies with time.

Reininger et al.[(4)] reported that platelets adhere to the surface of vWF-coated glass at discrete adhesion points, which have an area of 0.05–0.1 μm^2. In another experiment, immunofluorescence microscopy after staining with anti-GPIbα antibody showed that GPIbα localized to 3–5 spots on the platelet surface[(3)]. Although the density of GPIbα in localized regions has not been quantified, it is considered to be several times greater than that in non-localized region. GPIbα localization on platelet surface has the possibility to

*Received 10 Dec., 2011 (No. 11-0763)
[DOI: 10.1299/jbse.7.275]

greatly impact platelet adhesion, because the area of the localization region is comparable to the discrete adhesion points reported by Reininger et al.

In this study, we performed kinetic Monte Carlo (kMC) simulation[5] to evaluate the adhesion force between a platelet and vessel wall with respect to the primary aggregation of platelets. We stochastically determined the number of bonds between GPIbα and vWF by kMC simulation. Furthermore, we discuss the effect of GPIbα localization on the adhesion force of platelets. We aimed to develop a multiscale simulation scheme of thrombus formation. This kMC simulation can bridge the molecular-scale analysis of protein interactions and continuum-scale analysis of blood flow.

2. Methods

The adhesion site between platelets and vessel walls where platelet GPIbα molecules interact with the spherical vWFA1 domain is schematically shown in Fig. 1. Although unbound GPIbα molecules can diffuse onto the platelet cell membrane, vWFA1 domains are fixed on the vessel wall. If unbound GPIbα migrates to the reaction area around unbound vWFA1, GPIbα and vWFA1 form a bond at a rate of k_f. Once a GPIbα molecule binds to a vWFA1 domain, the GPIbα is fixed on the platelet cell membrane. Existing GPIbα–vWF bonds break at a rate of k_r. In this model, bonds are assumed to behave like stretched springs under force loading f_i that follow Hookean elasticity as follows:

$$f_i = k(l_i - l_0) \tag{1}$$

where k is the spring constant, l_i is the distance between platelet membrane and vessel wall, and l_0 is the equilibrium length of the bond. The adhesion force between a platelet and vessel wall is then expressed as:

$$F_{total} = \sum_{i=1}^{N_b} f_i \tag{2}$$

where N_b is the number of bonds. The number of bonds is stochastically calculated according to the kMC method by using the rates of bond formation, breakage, and GPIbα diffusion.

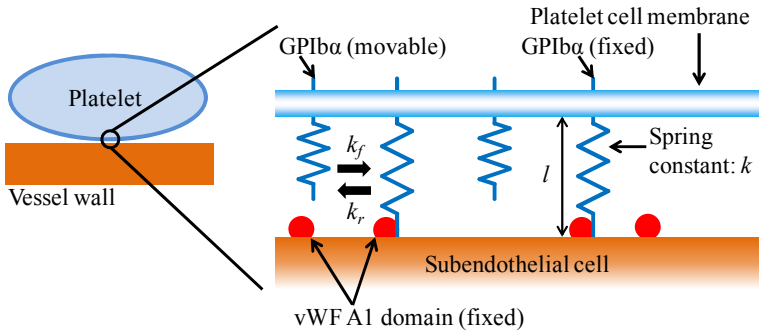

Fig. 1 Schematic illustration of the platelet–vessel wall contact surface

The kMC model was developed to evaluate the numbers of GPIbα–vWF bonds over time as well as the effect of GPIbα localization on the adhesion force between a platelet and vessel wall. A two-dimensional lattice with the periodic boundary condition was used to represent the platelet cell membrane and cell surface molecules. Fig. 2 is a schematic representation of the structure of the kMC lattice model. Simulations were performed on a 750 × 750 square lattice, with a lattice spacing of 2 nm that contained 4000 GPIbα. The GPIbα–vWF reaction areas were located around unbound vWFA1 domains with an area of 4 nm^2, which corresponds to one lattice cell. The calculation area corresponds to approximately 20% of the surface area of a platelet. There are up to 3600 vWF subunits on

a vessel wall with an area equivalent to the calculation region[6]. In this model, 3600 vWFA1 domains were placed uniformly in the area. Although the cause of GPIbα localization on the membrane is unknown, we assigned low-diffusivity regions in the center of the calculation region with the area of 0.09 μm^2 to simulate GPIbα localization. This was done by assuming that GPIbα localization occurs because of high-viscosity regions in the cell membrane, such as lipid rafts, which are cholesterol- and sphingolipid-rich membrane domains. The number density ratio of the GPIbα-localized and normal areas was assumed to be 2–10.

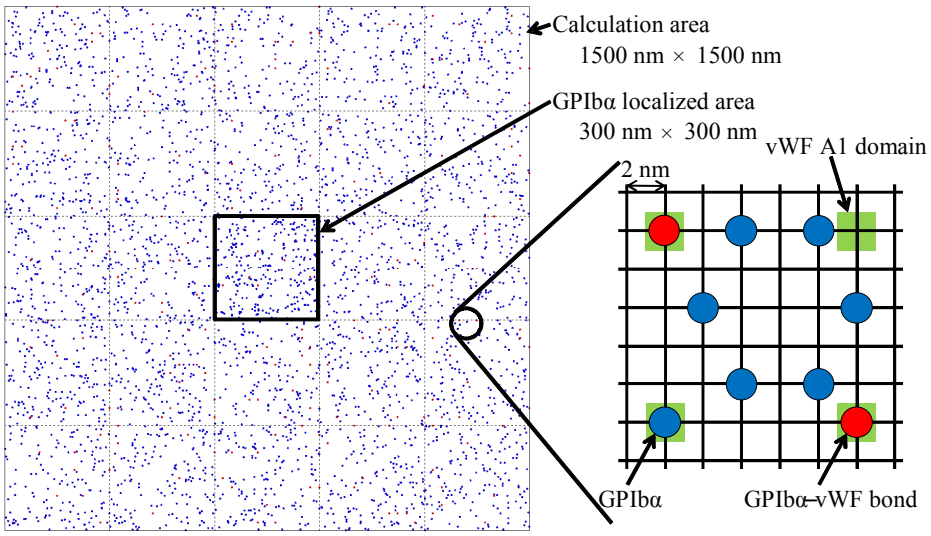

Fig. 2 kMC lattice model of a platelet surface

Simulations were initiated by placing GPIbα molecules on the lattice and then run by randomly choosing a single GPIbα and the probability-based selection of an event to occur at each time step. Possible events included GPIbα migration, bond formation, and bond breakage. The rates of the following 3 events were characterized for each GPIbα molecule: k_f for the formation of a new bond, k_r for the breakage of an existing bond, and k_d for the migration of GPIbα to the neighboring lattice point. The kMC simulations were performed by repeating the following 2 procedures: (i) a particular event of a particular GPIbα molecule was selected according to a random number and the event occurred; (ii) the time step, Δt, was also determined according to a random number, ρ, to update the simulation time by using the total rate R_{tot} in the form[5].

$$\Delta t = \frac{\ln(\rho)}{R_{tot}} \tag{3}$$

We employed the kinetic model by Dembo et al.[7] to express the transition rates of bond formation and breakage. Applying the transition state theory, k_f and k_r can be expressed in as follows:

$$k_f = k_f^0 \exp\left\{\frac{-k_{ts}(l_i - l_0)^2}{2k_bT}\right\} \tag{4}$$

$$k_r = k_r^0 \exp\left\{\frac{(k - k_{ts})(l_i - l_0)^2}{2k_bT}\right\} \tag{5}$$

where k_f^0 and k_r^0 are the unstressed reaction rates, k_{ts} is the transition state spring constant, k_b is the Boltzmann constant, and T is the absolute temperature. In this study, all simulations were run with T = 310 K. The values of k_r^0 and k were obtained from the results of an optical tweezers experiment involving a single GPIbα–vWFA1 bond[8]. Because it is difficult to determine k_f^0, the equilibrium constant K_{eq} was defined as a ratio of unstressed

reaction rates as follows:

$$K_{eq} = \frac{k_f^0}{k_r^0} \tag{6}$$

Simulations were conducted by varying K_{eq} in the range from 10^1 to 10^5.

The transition rate of diffusion, k_d, was calculated using the translational diffusion coefficient of the membrane, D. For a single particle exhibiting Brownian diffusion on a tetragonal lattice, the rate of a particle moving at least 1 lattice spacing, d_l, can be given as follows:

$$k_d = \frac{4D}{d_l^2} \tag{7}$$

The diffusion coefficient for a low-diffusivity localized region, D_{loc}, was assumed to be 1×10^{-12} cm^2/s. This value is consistent with the lower limit of cell membrane diffusivity for membrane receptors[9]. The ratio of diffusion coefficient for high-diffusivity regions to that for low-diffusivity regions, γ_{diff}, is calculated by considering transboundary movement of GPIbα as follows:

$$\gamma_{diff} = \frac{D_{n-loc}}{D_{loc}} = \frac{\gamma_{dens}\left(1-d_{n-loc}\right)}{1-\gamma_{dens}d_{n-loc}} \tag{8}$$

where $D_{n\text{-}loc}$, γ_{dens}, and $d_{n\text{-}loc}$ are the diffusivity for high-diffusivity non-localized regions, the ratio of the occupancy in localized to non-localized regions, and the occupancy in non-localized regions, respectively. The number density ratio was controlled through the diffusivity ratio by using Eq. (8).

3. Results and Discussion

3.1. GPIbα localization

First, kMC simulation was conducted without GPIbα–vWF interaction to confirm the control of GPIbα localization. Only the diffusion event of GPIbα molecules was included in the kMC lattice model shown in Fig. 2 by setting k_f and k_r to 0. The snapshots of GPIbα distribution on the kMC lattice model for a platelet surface when γ_{dens} = 5 are shown in Fig. 3(a)–(c). Fig. 3(d) shows the GPIbα number densities of localized and non-localized regions normalized by that of a uniform distribution. The diffusion coefficients were set to D_{loc} = 1.00×10^{-12} (cm^2/s) and $D_{n\text{-}loc}$ = 5.13×10^{-12} (cm^2/s) by using Eq. (8). The rates of GPIbα diffusion in localized and non-localized regions were determined by Eq. (7) using the values of D_{loc} and $D_{n\text{-}loc}$, respectively. Although the simulation was started with the uniform distribution of GPIbα shown in Fig. 3(a), GPIbα localization appeared in the center of the calculation area as the simulation progressed (Fig. 3(b)). Moreover, GPIbα localization was clearly observed at equilibrium (Fig. 3(c)). In this model, GPIbα molecules stayed longer in high-viscosity regions because of the low diffusion rate and consequently the number density of GPIbα increased, resulting in the formation of the localization area. The normalized number densities at equilibrium state (Fig. 3(d)) are approximately 4.3 and 0.86 for localized and non-localized regions, respectively. These results confirm that the ratio of the number density of GPIbα in localized regions to that in non-localized regions was controlled to be 5.

3.2. GPIbα–vWF interaction

To evaluate k_{ts}, the unbinding force distributions for various k_{ts} values were calculated using the kMC method and the results were compared with the experimental results. Kim et al.[8] investigated the force at which GPIbα and vWFA1 dissociated at different laser trap pulling rates (5–40 nm/s). They found that at pulling rates exceeding 20 nm/s, the

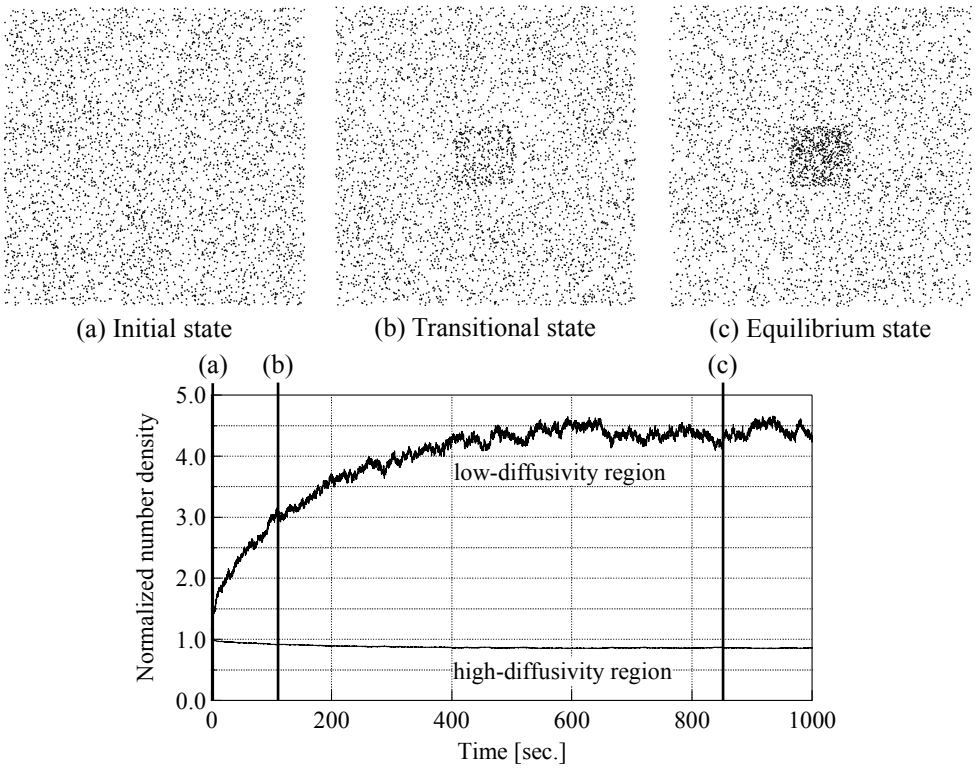

(d)Normalized number density of GPIbα molecule

Fig. 3 (a)–(c) Snapshots of GPIbα diffusing on a platelet membrane. Each dot corresponds to single GPIbα molecule. (d) Number densities of GPIbα molecule at low-diffusivity localized region and high-diffusivity non-localized region normalized by initial state density. (γ_{dens} = 5, D_{loc} = 1.00 × 10^{-12} (cm^2/s), $D_{n\text{-}loc}$ = 5.13 × 10^{-12} (cm^2/s), $k_f = k_r = 0$)

distribution of dissociation forces is clearly bimodal because of the 2 different dissociation pathways. In this study, only the first pathway, which has the same mechanism as that at lower pulling rates, was considered.

Fig. 4 is a schematic illustration of the calculation model for the experiment by Kim et al. In this model, only the bond breakage event was included for 10000 GPIbα–vWF bonds. Simulations were conducted from $l = l_0$ with updating l–l_0 in Eq. (5) according to the pulling rate until all the bonds broke. The unbinding force distributions were obtained from the unbinding distance distributions of GPIbα–vWF bonds by using Eq. (1). The unbinding force distributions normalized by the greatest number of bond breakages shown in Fig. 5 are corroborated by the experimental results when $k_{ts} = 0.9\ k$.

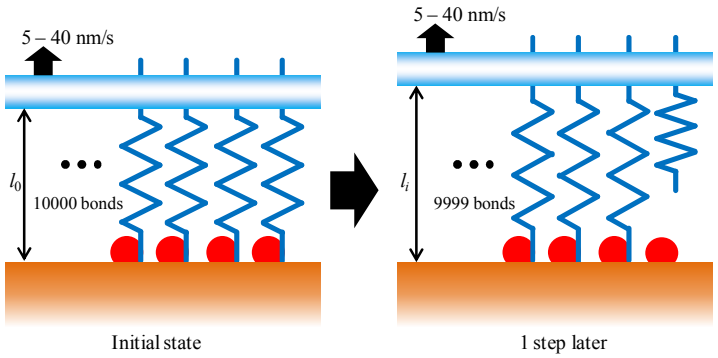

Fig. 4 Schematic illustration of the calculation model for the experiment by Kim et al.[8]

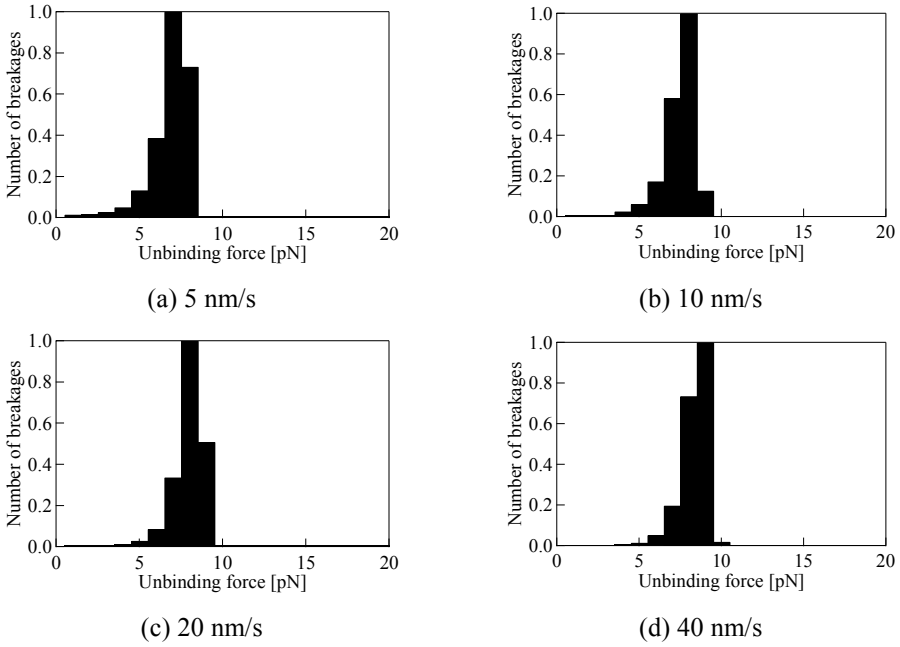

Fig. 5 Unbinding force distribution of single GPIbα–vWFA1 bond at different pulling rates between 5 and 40 nm/s.
(k = 0.1 [pN/nm], k_{ts} = 0.09 [pN/nm], k_r^0 = 0.0027 [s^{-1}])

Table 1 Parameter values for the rates of GPIbα–vWF bond formation, breakage, and GPIbα diffusion.

Parameter	*Value*	*Reference*
k (pN/nm)	0.1	(8)
k_{ts} (pN/nm)	0.09	
k_r^0 (s^{-1})	0.0027	(8)
K_{eq} (-)	10^1–10^5	
D_{loc} (cm^2/s)	10^{-12}	(9)
d_l (nm)	2	
T (K)	310	

3.3. Platelet–vessel wall interaction

To investigate the static response of the adhesion force of platelets with respect to the different ratios of localized number density, simulations were conducted using number density ratios of 2, 5, and 10 until equilibrium for GPIbα distribution and the number of bonds was reached. The time-averaged adhesion force was obtained for the fixed distance between vessel walls and platelets. The set of parameters used in the simulation is shown in Table 1. Simulations were conducted from l–l_0 = 0 to 50 (nm) at 1 nm intervals. The snapshots around the GPIbα-localized region in the case of γ_{dens} = 5 at equilibrium are shown in Fig. 6. The red dots represent GPIbα molecules bound to vWFA1, while blue dots represent unbound GPIbα molecules. Although most GPIbα molecules bound to the vWFA1 domain at l–l_0 = 0 (Fig. 6(a)), the number of bonds decreased with increasing l–l_0 (Fig. 6(b)); bonds rarely existed at l–l_0 = 30 nm (Fig. 6(c)). The profiles of adhesion force between a platelet and vessel wall were calculated using Eq. (2) and are shown in Fig. 7. Cases (a), (b), and (c) correspond to the conditions with number density ratios of 2, 5, and

10, respectively. Case (d) corresponds to the number density ratio of 5 and 25% of the vWF number density of other cases. The solid line in the figure indicates the adhesion force in the localized high-number density region (0.09 μm^2), and the dotted line corresponds to the averaged adhesion force in the low-number density region (0.09 μm^2). In cases (a)–(d) shown in Fig. 7, the total amount of adhesion force initially increased linearly with increasing platelet–wall distance because GPIbα–vWF binding provides linear restoring force. The force then starts decreasing beyond a certain distance because the decrease in the association rate k_f and increase in the dissociation rate k_r reduce the number of bindings. The drastic decrease in the total binding force is due to the rapid decrease in the association rate as shown in Fig. 8. The location with the maximum value moves in the right direction in Fig. 7 because larger K_{eq} values results in larger k_f^0 values, which can sustain more binding sites.

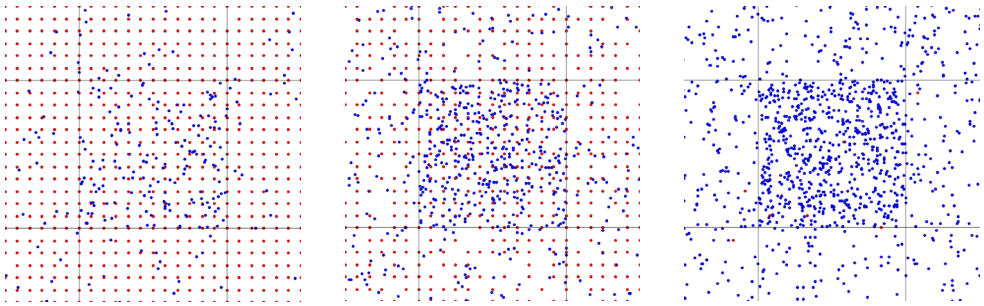

(a) $l–l_0 = 0$ (b) $l–l_0 = 20$ nm (c) $l–l_0 = 30$ nm

Fig. 6 Snapshots of the center of the calculation area. The framed square is the GPIbα-localized region. Blue dots: unbound GPIbα; red dots: bound GPIbα ($\gamma_{dens} = 5$, $K_{eq} = 1 \times 10^5$)

As shown in Fig. 7, the location of the peak value of adhesion force depends on the localization of GPIbα molecules. This tendency is stronger when there are high number density ratios in localized and non-localized regions. This is because the number of non-binding vWF increases with increasing distance and the number density of GPIbα molecules within binding site have a larger influence on the total number of bindings in interactions at larger distances. As shown in Fig. 9, increasing the distance increases the ratio of the number of bindings between localized and non-localized areas. These results indicate that the localization of GPIbα strongly influences platelet–wall interactions, especially when the platelets are away from the vessel wall.

The ratio of maximum adhesion force between localized and non-localized regions is shown in Fig. 10. When the equilibrium constant is large, the adhesion force is not strongly dependent on the number density of GPIbα. This is because most vWF is bound to GPIbα. In contrast, when the equilibrium constant is small, i.e., a small association rate, the adhesion force is strongly dependent on the number density ratio between localized and non-localized regions. For example, when $K_{eq} = 10$, the ratio of the adhesion force is close to the value of the number density ratio of GPIbα. This is because the difference of the number density of GPIbα molecules within vWF binding site impacts the difference of the number density of bonds when the number density of non-binding vWF is large. Furthermore, when the number density of vWF is small, although the total adhesion force decreases, the ratio of the number of bonds between localized and non-localized regions is almost the same as that for the large number density cases and the vWF density is insensitive to the influence of GPIbα localization.

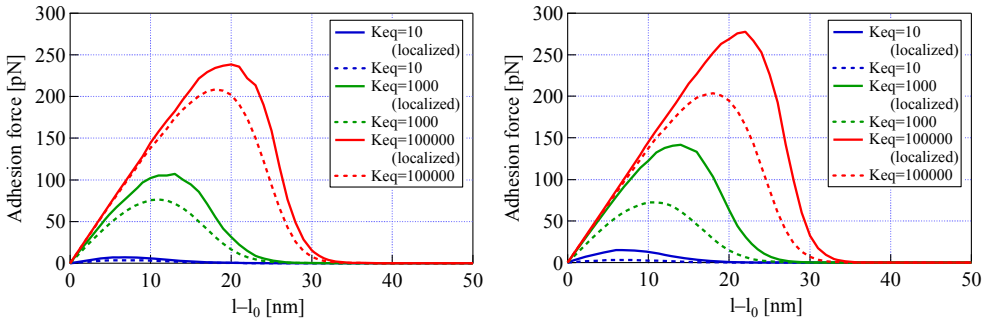

(a) ratio: 2 (b) ratio: 5

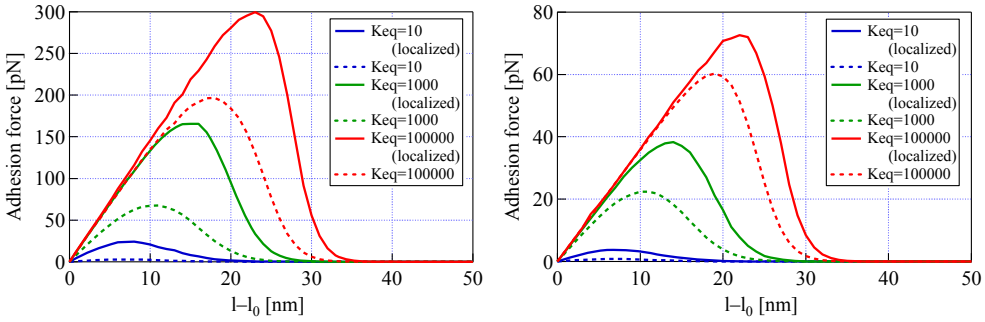

(c) ratio: 10 (d) ratio: 5 (1/4 vWF number density)

Fig. 7 Profiles of the adhesion force between a platelet and vessel wall. (Parameter values are shown in Table 1)

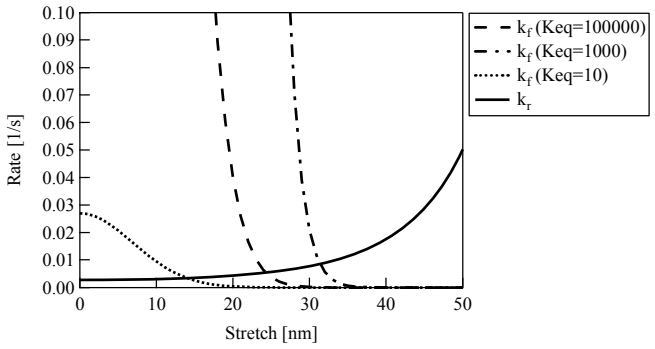

Fig. 8 Transition rates of GPIbα–vWF bond formation (k_f) and breakage (k_r).

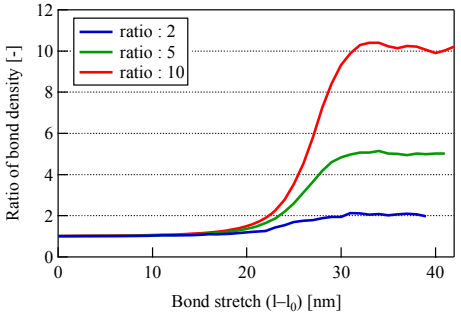

Fig. 9 Ratio of the number density of GPIbα–vWF bond vs. bond stretch. ($K_{eq} = 1 \times 10^5$)

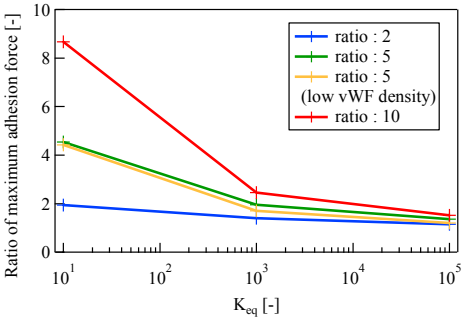

Fig. 10 Ratio of the maximum adhesion force of GPIbα–vWF bond vs. equilibrium constant.

4. Conclusion

The behavior of GPIbα on a platelet membrane was investigated using the kMC method. We developed the method to bridge the protein scale to the blood flow scale, which is related to the multiscale simulation of the early thrombus formation process. GPIbα molecules were localized on a platelet surface by designating a low-diffusivity region in the platelet cell membrane. The formation and breakage model of GPIbα–vWF bonds were constructed to reproduce experimental results. Next, we evaluated the adhesion force between a platelet and vessel wall, which was determined according to the number of bonds as well as the binding force of a single GPIbα–vWF bond, under static conditions. The adhesion force curves with respect to the distance between the platelet and vessel wall were convex upward. The kMC results indicate the possibility that the localization of GPIbα on a platelet surface significantly affects platelet–vessel wall interactions when the rate of GPIbα–vWF bond formation is low.

Acknowledgement

We gratefully acknowledge S. Goto, S. Ii, T. Koyama, Y. Nanazawa, S. Noda, N. Shimamoto, K. Sugiyama, Y. Sunaga, N. Tamura, and H. Yokota for their helpful discussions during group meetings for thrombosis simulator development in the Integrated Simulation of Living Matter (ISLiM) project. This study was supported by ISLiM, a part of the Development and Use of the Next-Generation Supercomputer Project of the Ministry of Education, Culture, Sports, Science, and Technology (MEXT) of Japan.

References

(1) Coller, B.S., Peerschke, E.I., Scudder, L.E. and Sullivan, C.A., Studies with a Murine Monoclonal Antibody That Abolishes Ristocetin-Induced Binding of von Willebrand Factor to Platelets - Additional Evidence in Support of GPIb as a Platelet Receptor for von Willebrand Factor, *Blood*, Vol.61, No.1(1983), pp.99-110.

(2) Goto, S., Salomon, D.R., Ikeda, Y. and Ruggeri, Z.M., Characterization of the Unique Mechanism Mediating the Shear-Dependent Binding of Soluble von Willebrand Factor to Platelets, *Journal of Biological Chemistry*, Vol.270, No.40(1995), pp. 23352-23361.

(3) Goto, S., private communication, June 17, 2010.

(4) Reininger, A. J., Heijnen, H. F. G., Schumann, H., Specht, H. M., Schramm, W. and Ruggeri, Z. M., Mechanism of Platelet Adhesion to von Willebrand Factor and Microparticle Formation under High Shear Stress, *Blood*, Vol.107, No.9(2006), pp.3537-3545.

(5) Fichthorn, K.A. and Weinberg, W.H., Theoretical Foundations of Dynamical Monte Carlo Simulations, *Journal of Chemical Physics*, Vol.95, No.2(1991), pp.1090-1096.

(6) Siedlecki, C.A., Lestini, B.J., KottkeMarchant, K., Eppell, S.J., Wilson, D.L. and Marchant, R.E., Shear-dependent Changes in the Three-dimensional Structure of Human von Willebrand Factor, *Blood*, Vol.88, No.8(1996), pp.2939-2950.

(7) Dembo, M., Torney, C.D., Saxman, K. and Hammer D., The Reaction-Limited Kinetics of Membrane-to-Surface Adhesion and Detachment, *Proceeding of the Royal Society B*, Vol.234, No.1274(1988), pp.55-83.

(8) Kim, J., Zhang, C.Z., Zhang, X.H. and Springer, T.A., A Mechanically Stabilized Receptor - Ligand Flex-bond Important in the Vasculature, *Nature*, Vol.466, No.7309(2010), pp.992-997.

(9) Kusumi, A., Sako, Y. and Yamamoto, M., Confined Lateral Diffusion of Membrane - Receptors as Studied by Single-Particle Tracking (Nanovid Microscopy) - Effects of Calcium-Induced Differentiation in Cultured Epithelial Cells, *Biophysical Journal*, Vol.65, No.5(1993), pp.2021-2040.